35th Annual International Conference of the IEEE EMBS
Osaka, Japan, 3 - 7 July, 2013

# A Novel Approach for Deriving Global Activation Maps from Non-Averaged Cardiac Optical Signals

Richard D. Walton, Olivier Bernus, and Rémi Dubois

*Abstract*— **Cardiac arrhythmias are often characterized by non-repetitive complex activation sequences. The properties of electrical activity in cardiac tissue, such as activation time (AT), can be accurately determined using optical imaging of electrical signals using voltage-sensitive dyes. The electrical AT of optical action potentials is known to accurately correlate with the time of the maximal derivative ($dF/dt_{max}$) of the upstroke of ensemble averaged optical signals. The sensitivity of $dF/dt_{max}$ to noise is therefore problematic for mapping AT from non-repetitive activity.**

**Here we experimentally evaluated a novel method to determine activation times (AT) from non-averaged epicardial optical signals. The method depends upon the time delays of activation between adjacent pixels developing a global AT map, as opposed to measuring local AT from each pixel independently based on $dF/dt_{max}$.**

**ATs from $dF/dt_{max}$ and global AT maps of non-ensemble averaged signals were correlated with averaged signals. Global ATs improved linear correlation coefficients and accuracy of AT patterns. Furthermore, global AT maps were significantly more robust at reproducing AT maps between consecutive stable beats.**

**The proposed method of global AT mapping will potentially enable accurate mapping of non-repetitive propagation during arrhythmias.**

## I. Introduction

Cardiac arrhythmias are characterized by abnormal propagation pathways in the heart. The spatial patterns of arrhythmias are often associated with, single or multiple focal sources [1]. Mapping the activation sequence of sustained and stable propagating waves enables identification of origins susceptible to spontaneous firing or regions of impaired conduction [2]. Electrical recording of the activation sequence is typically acquired through sequential point-by-point measurements, which is limited to stable and sustained activation sequences. Alternatively, epicardial multi-electrode arrays offer high temporal resolution but typically with spatial resolution in excess of 5 mm. However, *ex vivo* electrophysiological studies permit the use of optical imaging techniques that simultaneously acquire optical signals from multiple sites of cardiac tissue with superior spatio-temporal resolution.

This work was supported in part by the ESPRC under grant EP/F065574/1 (to R. D. Walton and O. Bernus), by the Agence Nationale de la Recherche under grant ANR-10-IAHU-04, by the Fondation Lefoulon Delalande (to R. Walton) and by the Marie Curie under grant FP7-PEOPLE-2011-IEF-300299 (to R. Walton).

R. D. Walton, O. Bernus and R. Dubois are with IHU-LIRYC, Université de Bordeaux, Bordeaux 33000, France and with the Unité Inserm 1045, Centre de Recherche Cardio-Thoracique, Université Bordeaux Segalen, Bordeaux 33076, France. R. D Walton, and O. Bernus are with Faculty of Biomedical Sciences, Multidisciplinary Cardiovascular Research Centre, University of Leeds, Leeds LS2 9JT, UK.

Optical mapping of electrical activity in cardiac tissue is achieved using voltage-sensitive fluorescent dyes. The optical signal is proportional to changes in the transmembrane potential. However, in three-dimensional (3D) tissue, it is represented by a weighted sum of single-cell cardiac signals over a certain volume [3, 4]. This volume is determined by the level of scattering and absorption of excitation and fluorescent signals, which depends on the wavelength of excitation and fluorescent light, tissue thickness and other geometric factors and recording conditions [4, 5]. Consequently, the local optical upstroke is relatively prolonged compared with the electrical AP from the same location on the tissues surface [3, 4]. Furthermore, the morphology of the optical upstroke varies considerably depending on the orientation of the wave front with respect to the imaged tissue surface [6]. The question that therefore arises is the determination of the true epicardial activation time based on optical signals. We recently showed that the time of the maximal derivative ($dF/dt_{max}$) of the optical upstroke corresponds accurately to the time of local electrical activation [7]. However, $dF/dt_{max}$ is sensitive to noise and is therefore often applied in conjunction with significant filtering and ensemble averaging for repetitive activation sequences during pacing [8].

Conventionally, the ATs from optical signals are derived in each pixel independently of neighboring pixels. Dubois *et al.* [9] proposed a method to determine ATs of electrocardiograms based on the local delays between adjacent electrodes. Therefore, a global AT map is derived between all adjacent conducting sites measured without explicitly computing the local AT. This method was considerably more robust against noise. Moreover, the AT sequence was reproducible between sequential beats assigned with random noise.

The current study assessed the applicability of the global AT approach by Dubois *et al.* [9] to cardiac optical signals, which inherently have variable upstroke morphologies between neighboring pixels. We present the first results using such global AT method applied to optical signals developed for application with non-ensemble averaged signals. Here, global AT maps from several consecutive stimulated beats with point-source activation patterns were compared against the conventional $dF/dt_{max}$ approach. Both methods were correlated with $dF/dt_{max}$ of the ensemble-averaged signal, which has previously been validated to correspond to the surface electrical activation time. Statistical comparisons of AT differences between non-averaged and averaged signals and the beat-to-beat variability of each method were determined.

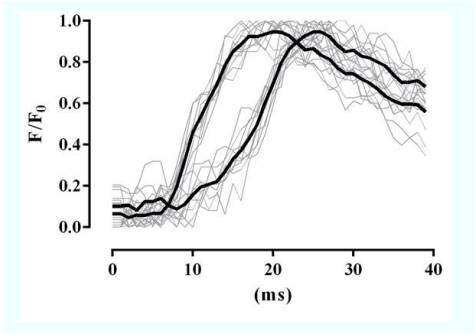


Figure 1. Averaged and non-averaged optical upstrokes. Non-averaged upstrokes from two pixels (locations are indicated in Fig 2) from consecutive propagating APs are aligned by stimulus time (grey lines). Signals are overlaid by the ensemble averaged optical signal for comparison (thick solid lines).

## II. METHODS

### A. Heart Preparation

Experiments were conducted using male Wistar rats (200g, n = 4) in accordance with the UK Animals (Scientific Procedures) Act 1986. Hearts were excised and the aorta cannulated for horizontal perfusion in Langendorff mode with a bicarbonate buffered saline solution containing (mmol/L): NaCl, 130; $NaHCO_3$, 24; $NaH_2PO_4$, 1.2; $MgCl_2$, 1; glucose, 5.6; KCl, 4; $CaCl_2$, 1.8; oxygenated with 95% O2/5% CO2, pH 7.4. Perfusion was maintained at 7ml/min and at a temperature of 37°C. The perfusion was supplemented with 10 μM blebbistatin for mechanical uncoupling of the myocardium.

### B. Optical Mapping

The tissue was stained with potentiometric dye DI-4-ANEPPS (50 μg/ml bicarbonate buffered saline solution) via the perfusate at the beginning of the experiment. Bipolar electrodes were used to stimulate the ventricles at basic cycle lengths of 160 ms. Hearts were allowed to stabilize for 30 minutes while continuously pacing before measurements were made. Optical recordings were acquired through a high-frame-rate charge-coupled device video camera (SciMeasure Analytical systems, GA, USA) mounted with a lens (focal length 12 mm, 1:0.8 aperture ratio; Computar, London, UK). Excitation light from monochromatic LEDs, 530 nm, (Cairn Research Ltd, Kent, UK) illuminated the epicardial surface. Emission light from DI-4-ANEPPS was filtered through a broadband 700DF50 filter. Images (80x80 pixels) with pixel dimensions of 0.25x0.25 mm were acquired at 1000 frames per second.

### C. Processing of Optical Signals

Optical recordings were separated in the time-dimension by markers of stimulus time to isolate the first 11 APs. For comparison with non-averaged data, the 11 APs were ensemble averaged. Averaged and non-averaged APs were filtered using a Savitzky-Golay filter that is able to estimate directly a smoothed derivative signal from a raw signal. This was achieved by locally interpolating AP signals by a polynomial approximation. A smoothing window of 5 ms was used with a polynome of order 1 (i.e. by a linear approximation).

The signal was then oversampled using spline interpolation to achieve a temporal resolution of 0.1 ms. The smoothed action potential is then recovered by integration of the filtered signal. A spatial window of pixels (18x17) localized to the center of the tissue that incorporated the sites of stimulation but avoided edges of tissue, which are often associated with motion artifact leading to false estimates of AP properties, was used for analysis. For each method, ATs were estimated from the first 30 ms of each image as the total activation time of the ventricles was found not to exceed 25 ms in ensemble averaged movies.

### D. Estimating Optical Activation Times

The current proposed methodology for measuring optical activation times on non-averaged data was compared with the conventional $dF/dt_{max}$ approach. $dF/dt_{max}$ was defined as the time of the peak of the smoothed derivative curve. The novel method hereby proposed for estimating global ATs from optical action potentials was previously validated for cardiac electrical signals [9]. In brief, the core of this methodology is to determine the delay in activation between neighboring pixels during a single propagation of the depolarizing wave front. Global AT is an estimate of AT at each pixel, however, this estimation is global in the sense that it is computed in order to optimally fit local delays between pixels at all locations. The global AT algorithm uses estimates of local activation delays, which form the inputs of a linear system of equations, leading to a map of global AT. Here, the previous method [9] was adapted for optical AP signals by assuming equal magnitudes of transmembrane potential depolarization in all regions and therefore optical signal amplitudes were first normalized. For each pixel, the signal amplitude of $dF/dt_{max}$ was identified and the delay to neighboring pixels in horizontal, vertical and diagonal directions derived. Each pixel is associated with its own $dF/dt_{max}$ and therefore two delays are determined for each pixel-pair. The resultant delay between each pair of pixels is determined as the mean of those delays. For a detailed description of the computation of this method see [9].

### E. Analysis and Statistics

The accuracies of each method for estimating AT from non-averaged data were compared against the $dF/dt_{max}$ of the ensemble averaged AP ($dF/dt_{average}$), which was recently validated as an accurate measure of the true electrical AT [7]. The GAT method derives ATs from delays between signals of neighboring pixels. The reported ATs are therefore defined with respect to the AT of the earliest pixel. As such, AT maps from each method were subtracted by their minimum AT before all comparisons.

Estimations of AT across all pixels from non-averaged signals were plotted against ATs derived from corresponding pixels of averaged signals. Correlations between signals were assessed by linear regression analyses. The variance of AT estimates from non-averaged signals was determined by the standard deviation of the differences of AT ($t_{diff,ij}$) between non-averaged ($t_{F,single,ij}$) and the averaged signals, as determined by

$$t_{F,single,ij} - dF/dt_{average,ij} = t_{diff,ij}, \quad (1)$$

where $i$ and $j$ are pixel co-ordinates that range from 0 to N-1 of pixels in each direction.

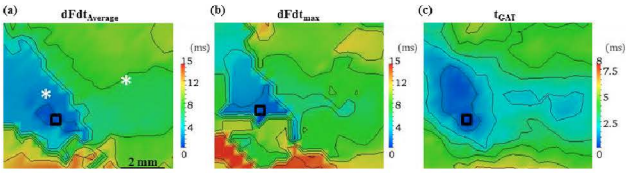


Figure 2. Epicardial activation patterns derived from ensemble averaged and non-averaged optical signals. Panels (a) and (b) are dF/dt$_{max}$ maps derived from averaged and non-averaged optical signals, respectively. Isochrones are spaced 2ms apart. (c) A global AT map from non- averaged signals. Isochrones are spaced 1ms apart. The pixel corresponding to the earliest activation is indicated in each activation time (AT) map by a black box. Colour scales are independent for each map.

The disparity of the AT estimated by each method from non-averaged signals were investigated by assessment of the absolute difference of AT ($|t_{diff,ij}|$) between non-averaged and averaged signals, as shown by

$$|t_{F,single,ij} - dF/dt_{average,ij}| = |t_{diff,ij}|. \quad (2)$$

Finally, the beat-to-beat variability ($var_{t,ij}$) of ATs between sequential beats of stable paced activity was quantified for ATs from each method. This was determined from the standard deviation of $t_{diff,ij}$ ($\sigma(t_{diff,ij})$) normalized by the mean ($\bar{\chi}(t_{diff,ij})$)for each pixel across 11 consecutive beats as shown by

$$\sigma(t_{diff,ij})/\bar{\chi}(t_{diff,ij}) = var_{t,ij}. \quad (3)$$

Statistical differences between results from each AT method were determined by paired t-test, $p<0.05$.

## III. Results

Methods of deriving optical activation times were validated using optical signals recorded from controlled experiments whereby hearts were stimulated at constant basic cycle lengths to ensure reproducible sequential patterns of propagation. Fig 1 shows the non-averaged AP upstrokes from two pixels of a single optical recording aligned by stimulation time and overlaid. Variations of the activation pattern would expect to yield considerable variation in delays between rise times. However, rise times of non-averaged optical signals overlapped consistently for each pixel over 11 consecutive beats, despite significant noise. Also overlaid are the respective ensemble-averaged signals whereby noise was significantly reduced and upstrokes clearly defined with respect to dF/dt$_{max}$.

### A. *Qualitative comparison of AT maps*

Fig 2 shows the dF/dt$_{max}$ map of averaged optical signals that shows clearly defined sites of earliest activation and, in accord with previous studies [7], anisotropic patterns of propagation (Fig 2a). AT maps of non-averaged signals were shown to illustrate the level of correspondence with the averaged AT map for dF/dt$_{max}$ and global AT methods (Figs 2b and c, respectively). The range of ATs derived by dF/dt$_{max}$ from non-averaged signals was similar in magnitude to the averaged AT map. However, this method poorly reproduced the pattern of early activation. The location of the pixel with the earliest AT was shifted by 0.58 mm relative to the averaged AT map. Furthermore, the dF/dt$_{max}$ map was associated with increased lines of conduction slowing, illustrated by isochrones clustering in Fig 2b. In contrast, the global AT method, although had overall a reduced range of ATs, resembled more closely the directions of propagation and the site of earliest activation. The shift in the site of earliest activation was reduced to 0.31 mm using the global AT method (Fig 2c).

### B. *Linear correlations of AT between averaged and non-averaged signals*

Conformity of activation sequences between averaged signals and of non-averaged signals were analyzed using pixel-to-pixel comparisons and linear regression analysis. Representative pixel-to-pixel plots of ATs between dF/dt$_{max}$ of averaged signals and non-averaged signals using dF/dt$_{max}$ and global AT methods are shown in Figs 3a and 3b. The slopes, intercepts and linear correlation coefficients ($r^2$) of linear relationships are shown. Slopes were closer to 1 for the dF/dt$_{max}$ vs. the global AT method, where a slope of 1 indicates that the propagation delay between neighboring pixels across the AT map was preserved. However the intercept, an indicator of AT convergence at t=0 ms, was close to the temporal resolution of optical recordings (1 ms) for global AT but closer to 3 ms for dF/dt$_{max}$. Furthermore, the $r^2$ was markedly improved by global AT compared with dF/dt$_{max}$. Figs 3c, 3d and 3e show the Mean±SD of the slope, intercept and $r^2$, respectively, of linear relationships between all pairs of averaged and non-averaged optical images. Slopes for all individual comparisons were less than 1, but the Mean±SD of slopes for the global AT method were significantly less than for dF/dt$_{max}$, N=99, P<0.0001. In contrast, the Mean±SD of both the intercept and $r^2$ were improved significantly using the global AT method compared with dF/dt$_{max}$, N=99, P<0.0001.

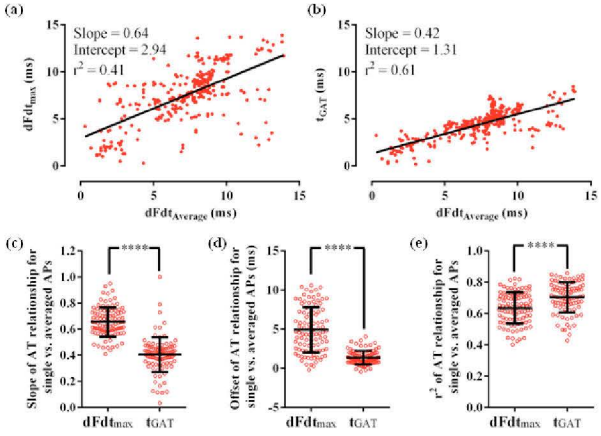


Figure 3. Correspondance among ensemble averaged and non-averaged optical activation times (AT). (a) Linear correlation between ATs of averaged signals and dF/dt$_{max}$ of non-averaged signals. A low $r^2$ and intercept relatively far from zero signify a poor correlation between averaged and non-averaged ATs. (b) Linear correlation between the global ATs of non-averaged signals and averaged ATs. Raw and Mean±SD values of slope (c), intercept (d) and $r^2$ (e) from individual AT maps, N=99. All significant differences were determined by unparied t-tests, P<0.0001.

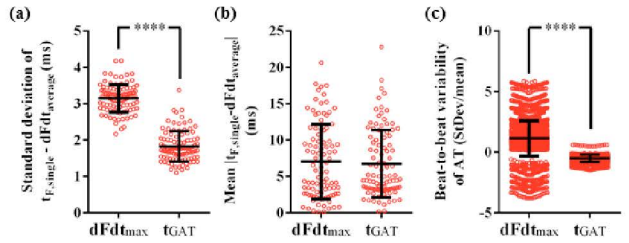


Figure 4. The variability and magnitude of activation time (AT) errors between non-averaged and ensemble averaged optical signals. (a) The standard deviations of the relative differences of AT between averaged and non-averaged signals derived by $dF/dt_{max}$ and global AT methods. Variance of AT error is reduced by using he global AT method. N=99. (b) Absolute mean difference of AT between averaged and non-averaged signals. The magnitude of AT error were equivalent between $dF/dt_{max}$ and global ATs methods. N=99. (c) Temporal variability of AT between consecutive reproducible beats for $dF/dt_{max}$ and global ATs. beat-to-beat ATs are reproduced with increased robustness using global AT compared with $dF/dt_{max}$. N=3598. All significant differences were determined by unparied t-tests, P<0.0001.

### C. *Spatial variance of AT error of non-averaged signals*

For each $dF/dt_{max}$ and global AT methods, the variance of non-averaged ATs around the averaged ATs was quantified by the standard deviation of AT differences from each image of AP recordings (1). The Mean±SD of variance across all images was compared between AT methods (Fig 4a). Global ATs were associated with significantly reduced variances of AT errors compared to $dF/dt_{max}$, N=99, P<0.0001. The magnitude of the mean error of ATs between non-averaged and averaged signals was determined as described in (3). Fig 4b shows that the Mean±SD of the absolute mean error was found not to significantly differ between $dF/dt_{max}$ and global ATs, P>0.05, N=98.

### D. *Beat-to-beat variability*

AT maps of consecutive APs were used to determine the beat-to-beat variability of ATs for $dF/dt_{max}$ and global AT methods. Beat-to-beat variance over 11 consecutive APs was calculated for each pixel and repeated for 9 independently recorded images (3). Fig 4c shows beat-to-beat variances calculated for each pixel and are overlaid by their Mean±SD for $dF/dt_{max}$ and global ATs. Global ATs were associated with significantly reduced beat-to-beat variability compared to $dF/dt_{max}$ N=3598, P<0.0001. Furthermore, the distribution of variance across all pixels was conserved between beats for global ATs, based on comparisons between the standard deviation of the mean variance (0.30 vs. 1.45).

## IV. Discussion

The present study proposes a novel approach to determine the activation sequence from non-ensemble averaged optical signals of cardiac electrical propagation. This method determines the sequence of activation based on delays between neighboring pixels, as opposed to interpreting the local AT from each pixel independently. The first experimental results using this method showed that it better reproduced the spatial organization of activation of ensemble averaged signals (high signal:noise ratio) from non-averaged signals susceptible to noise. This approach was found to have reduced spatial variation in ATs and, moreover, was found to reliably reproduce AT maps between consecutive activation patterns of stable paced activity compared to relying on $dF/dt_{max}$.

Although the global AT method proved robust at reproducing patterns of activation with minimal variability, ATs were progressively underestimated with a linear accumulation of error. We may partly explain this discrepancy based on the variability of the upstroke morphology. The amplitude of $dF/dt_{max}$ is dependent upon the orientation of the propagating wave front with respect to the imaged surface and is therefore variable across the epicardial surface of focal-source activation patterns. It is therefore reasonable to assume that average AT delays measured at the amplitudes of $dF/dt_{max}$ between adjacent pixels are different to the average difference measured between the $dF/dt_{max}$ of adjacent pixels.

Optical signals were subject to Savitsky-Golay temporal filtering to reduce noise prior to determining AT. This filter enables preservation of the morphology of the signal where other filters that are dependent on frequency thresholds would likely significantly modify the AP upstroke, which exhibits a relatively high frequency component due to a rapid change of transmembrane potential.

## V. Conclusion

The present study provides a novel method for AT mapping of non-averaged signals and potential for reliable AT mapping of non-repetitive activity during arrhythmias.

## References

[1] Robichaux, R.P., Dosdall, D.J., Osorio, J., Garner, N.W., Li, L., Huang, J., and Ideker, R.E.: 'Periods of highly synchronous, non-reentrant endocardial activation cycles occur during long-duration ventricular fibrillation', Journal of cardiovascular electrophysiology, 2010, 21, (11), pp. 1266-1273

[2] Haissaguerre, M., Shoda, M., Jais, P., Nogami, A., Shah, D.C., Kautzner, J., Arentz, T., Kalushe, D., Lamaison, D., Griffith, M., Cruz, F., de Paola, A., Gaita, F., Hocini, M., Garrigue, S., Macle, L., Weerasooriya, R., and Clementy, J.: 'Mapping and ablation of idiopathic ventricular fibrillation', Circulation, 2002, 106, (8), pp. 962-967

[3] Girouard, S.D., Laurita, K.R., and Rosenbaum, D.S.: 'Unique properties of cardiac action potentials recorded with voltage-sensitive dyes', Journal of cardiovascular electrophysiology, 1996, 7, (11), pp. 1024-1038

[4] Gray, R.A.: 'What exactly are optically recorded "action potentials"?', Journal of cardiovascular electrophysiology, 1999, 10, (11), pp. 1463-1466

[5] Bishop, M.J., Gavaghan, D.J., Trayanova, N.A., and Rodriguez, B.: 'Photon scattering effects in optical mapping of propagation and arrhythmogenesis in the heart', Journal of electrocardiology, 2007, 40, (6 Suppl), pp. S75-80

[6] Zemlin, C.W., Bernus, O., Matiukas, A., Hyatt, C.J., and Pertsov, A.M.: 'Extracting intramural wavefront orientation from optical upstroke shapes in whole hearts', Biophysical journal, 2008, 95, (2), pp. 942-950

[7] Walton, R.D., Smith, R.M., Mitrea, B.G., White, E., Bernus, O., and Pertsov, A.M.: 'Extracting surface activation time from the optically recorded action potential in three-dimensional myocardium', Biophysical journal, 2012, 102, (1), pp. 30-38

[8] Laughner, J.I., Ng, F.S., Sulkin, M.S., Arthur, R.M., and Efimov, I.R.: 'Processing and analysis of cardiac optical mapping data obtained with potentiometric dyes', American journal of physiology. Heart and circulatory physiology, 2012, 303, (7), pp. H753-765

Dubois, R., Labarthe, S., Coudière, Y., Hocini, M., and Haissaguerre, M.: 'Global and Directional Activation Maps for Cardiac Mapping in Electrophysiology', IEEE Conference Proceedings: Computing in Cardiology, 2012, In Press